International Research Journal of Innovations in Engineering and Technology (IRJIET)

ISSN (online): 2581-3048

Volume 7, Issue 12, pp 55-59, December-2023

https://doi.org/10.47001/IRJIET/2023.712007

Synthesis, Characterization and Photocatalytic Activity of MnO_2 and Magnetic Sand Composites

[1]Charity Musa, [2]Jeffrey T. Barminas, [3]*Shinggu D. Yamta, [4]Janyo Noseh Dahiru

[1,3,4]Department of Chemistry, Adamawa State University Mubi, PMB 25 Mubi, Adamawa State, Nigeria

[2]Department of Chemistry, Modibbo Adama University Yola, Adamawa State, Nigeria

*Corresponding Author's E-mail: shinggudy@gmail.com

***Abstract* - The synthesis of manganese oxide and magnetic sand nanocomposites was reported in this study. The MnO2 nanoparticles was synthesized using biological approach in which aqueous Cassia tora leaf extract was used to bioreduced potassium permanganate (KMnO4) to manganese oxide and characterized using Fourier Transformation Infrared (FTIR) spectroscopy, UV-visible spectrophotometer, XRD and SEM. The UV-visible spectrophotometer gave an absorption at 290 nm, while the crystalline size was obtained from XRD technique. Physical method was adopted for magnetics sand synthesis using Tema vibrating mill. This was achieved by Agate Moter before sieving through 63 microns' sieve. The formed magnetic sand was characterized using FTIR, XRD, X-ray fluorescent (XRF). The result of the XRD shows that the crystalline size of the particles. The XRF shows that the sand contains high percentage of SiO2 about 70.16%. The photocatalytic activities of manganese oxide and magnetic sand nanocomposites were carried out for the degradation of methyl orange. The result shows that the nanocomposite can be used for the degradation of methyl orange and can be reused for a series of cycles without a significant decrease in the degradation ability.**

Keywords: Synthesis, Characterization, Nanoparticles, Photocatalysis degradation.

I. INTRODUCTION

Nanotechnology has attracted a great deal of attention in the last decades as miniaturization and nanomaterial are often foreseen to be the key for a sustainable future. In a broadest sense, Nano chemistry makes use of the tools of synthetic and material chemistry to generate nanomaterial with size, shape and surface properties that can be designed to evoke a specific function with the aims to be utilized in a particular application/end use. Nanotechnology allows us to manipulate the matter on a molecular scale (much less than 100 nanometers), helping us to obtain valuable information for the synthesis of new materials with specific properties and with a high degree of reproducibility [1]. In this regard, an important part of the scientific community is currently focused on a very challenging and relevant research direction, which is the synthesis of novel nanostructured materials capable of absorbing the photonic energy coming from the sun with the aim of turning it into chemical or electrical energy [1]. Nanostructured materials have been extensively explored for the fundamental scientific and technological interests in accessing new classes of functional materials with unprecedented properties and applications [2]. Metal oxides play a very important role in many areas of chemistry, physical and materials science [3]. Metal oxides are formed as a consequence of co-ordination tendency of metal ions so that oxide ions form co-ordination sphere around metal ions and give rise to close packed structure. The different physical, magnetic, optical and chemical properties of metal oxides are of great interest to chemists because these are extremely sensitive to change in composition and structure. Extensive studies of this relationship leads to a better understanding of the chemical bond in crystal. The metal oxides are attracting special attention of scientists due to their easy mode of formation and multifunctional [3]. Photo-catalytic activity of many metal oxide nanoparticles such as Gd-doped $BiFeO_3$ have been evaluated and proven as efficient photo-catalysts for photo-catalytic degradation of methylene blue, methyl orange, organic pollutant, inhibiting bacteria growth, decomposition of NO_2 and photo-catalytic water splitting, owing to their ability to absorb ultraviolet radiation, due to their relatively high photo-catalytic activity, robust chemical stability, low cost and nontoxicity [3]. However, the amount of UV light they absorb is very small about 1% to 5% and it is believed that this can be improved by using other nanomaterial or blending two or more of the nanomaterial. Over the last decade there has been increased interest in semiconductor nanoparticles due to their potential applications in photo-catalysis, gas sensors, solar cells, UV light-emitters, electronic and optical devices, fuel cells and smart materials [3]. Specifically, much attention has been drawn towards their photo-catalytic properties because of their applications in environmental purification and decomposition of toxic and organic compounds. A key requirement for improving the photo-catalytic activity is to increase the specific surface area and enhance the crystallinity. These requirements are met by crystalline nanostructured materials. Several methods

International Research Journal of Innovations in Engineering and Technology (IRJIET)

ISSN (online): 2581-3048

Volume 7, Issue 12, pp 55-59, December-2023

https://doi.org/10.47001/IRJIET/2023.712007

including hydrothermal, sol-gel, chemical vapor deposition (CVD) and sputtering have been used to prepare metal oxide nanoparticles. For efficient photo-catalytic activity, nanomaterial need to be crystalline, that is, should be grown at high temperatures or at very slow rates [4]. The pollution of water and the environment at large by organic synthetic none degradable/decomposable materials such as phenol, methyl orange, rhodamine B has been of great concern causing cancer, skin, respiratory and digestive system diseases [5]. Phenols particularly when ingested affect central nervous system, cause loss of consciousness and collapse in both human and animals. The presences of these substances affect aquatic life since they make water to have a characteristic taste and colour [6]. Therefore, there is need to device a means of degrading or decomposing these substances into none harmful substances by the used of photo-catalyst which were safe for the environment. This research work thus aims at synthesize, characterize and determine photo-catalytic activity of MnO_2/Al_2O_3/Magnetic sand nanocomposite.

II. MATERIALS AND METHODS

All materials used are of analytical grades. FT-IR Spectrophotometer (Perkin Elmer) in the range of 4000-400cm-1, UV-visible spectrophotometer (Jenway 6405) in the range of 200-600 nm, XRD (Empyrean panalytical model), Scanning electron microscope (SEM, JEM 2100, JEOL, Japan).

A) Preparation of Cassia Toraleaf extract

Cassia Tora leaves were collected within the University and was identified in the Department of Botany, Adamawa state University. The aqueous extract was prepared by mixing 10 g of dried leaves powder with 100 mL of water (boiled and cooled distilled water) with constant stirring on a magnetic stirrer. The suspensions of dried leaves powder in water were left for 3 hours and were filtered through Whatman No. 1 filter paper. The filtrate was use immediately adopting the method of [7].

B) Synthesis of MnO_2 Nanoparticles

About 0.2 M aqueous solution of potassium per manganate ($KMnO_4$) was prepared and use for the synthesis of manganese nanoparticles. 5 ml of Cassia tora leaves extract was added into 50 ml of aqueous solution of 0.2 M potassium per manganate ($KMnO_4$) for reduction into MnO_2 and kept at room temperature for 30 min [8].

C) Preparation of Magnetic Sand Nanoparticles

Magnetic sand sample was prepared according to the method of [9], the magnetic sand sample was prepared by reducing the particles size to less than 63 microns using a Tema vibrating mill. This was done by the Agate Moter in the mill crushing the sample before sieving through 63 microns' sieve.

III. RESULTS AND DISCUSSIONS

A) UV-Visible spectroscope of MnO_2 nanoparticle

Nanoparticles in general have absorption characteristics in the UV–Visible region and the absorption intensity of nanoparticles generally increases with an increase in nanoparticles concentration [9]. In this study, MnO_2 nanoparticles synthesized showed characteristic absorption peak at 290 nm as shown in figure 3.1. Which is similar to the one reported by [10]. The characterization of MnO_2 nanoparticle using UV-Visible spectroscope gave a sharp absorption peak at 285 nm.

B) FTIR analysis of MnO_2, Magnetic Sand Composite and Cassia tora leaves

FTIR spectroscopy was carried out in order to ascertain the purity and nature of manganese oxide. Oxides and hydroxides of metal nanoparticles generally gives absorption peak in the finger print region i.e. below wavelength of 1000 nm arising from inter-atomic vibrations [11]. The bands at 809.59 cm^{-1} and 707.45 cm^{-1} found in the metal oxide correspond to the Mn–O bond (Table 1). Absorption peak observed at 3323.89 cm^{-1} and 3280.20 cm^{-1} present in the metal oxide and cassia tora leaf extract respectively may be due to OH stretching vibrations of water (Table 2). The absorption peaks at 2919.03 cm^{-1} observed in the Cassia tora leaf correspond to C-H bending, 2850.75 cm^{-1} C-H stretch of alkane (Table 3). The absorption band at 1614.44 cm^{-1} in the metal oxide and 1587.75 cm^{-1} in the Cassia tora leaf are assign to C=O of amide. The peaks at 1359.89 cm^{-1}, 1308.96 cm^{-1} of the metal oxide and 1247.83 cm^{-1} of the plant may be due to C-O stretching vibrations. While the absorption band at 1012.37 cm^{-1} in the plant is for CN stretching amine. This result is in agreement with that reported by [12]. In magnetic sand composite, the stretching vibration spotted around 774.92 cm^{-1} helps to tell about different forms of silica [13]. Consequently, the band at 774.92 cm^{-1} show that the silica is in the form of α-quartz. A sharp band was observed at 727.25 cm^{-1}. A plausible explanation for this observation is that the sand sample may have been contaminated with another mineral – Albite, which absorbs at a very closely to this – 727.25 cm^{-1}. Albite has the chemical formula $NaAlSi_3O_8$. Geochemical analysis from other study on the sample reveals that traces of Na in addition to Si and Al. This result lends credence to the explanation of the band observed at 727.25 cm^{-1}. A sharp peak was observed at 694.74 cm^{-1}. This absorption can be taken to represent Si-O symmetrical

International Research Journal of Innovations in Engineering and Technology (IRJIET)

ISSN (online): 2581-3048

Volume 7, Issue 12, pp 55-59, December-2023

https://doi.org/10.47001/IRJIET/2023.712007

bending vibration [14]. This is similar to bands at 694 cm^{-1}, 693 cm^{-1} and 695cm^{-1} reported by [14]. Further, the presence or absence of an absorption band at around 694.74 cm^{-1}, helps determine if the observed quartz is crystalline or amorphous. Amorphous silica do not absorb at this frequency, while crystalline silica do [14]. Following this, we infer that the quartz in the sand sample is in the crystalline form. Observation of a slight shift in position of the characteristic peak at 694.74 cm^{-1} may be due to associated minerals or crystal fault of the sample. An example of such associated mineral in this case is kaolinite. Without this interference, we may have observed absorption at 694.74 cm^{-1}. The band at 3749.71 cm^{-1}can be taken to represent OH stretching of crystalline hydroxyl. OH in crystalline hydroxyl of theoretical kaolin absorbs at 3645 cm^{-1} [14]. 1002.93 cm^{-1} absorption band can also be assigned to a yet to be named vibration in kaolin (kaolinite is the major constituent of kaolin). 1456.94 cm^{-1}can be regarded as the overtone band of a 727.25 cm^{-1} which represents the absorption band of a suspected associated mineral – Albite [14]. Furthermore, The FT-IR of Cassia tora leaves show the present of 7 peaks which correspond to OH; C-H bond stretching, OH of carboxylic acid, C-H of alkane C-O stretch of amide, C=O bending of amide, C-N stretch of aliphatic amine.

Table 1: FT-IR data of MnO_2

Frequency cm^{-1}	Functional groups
3323.98	O-H
1614.44	C=O
1359.89	C-H
707.45	Mn-O

Table 2: FT-IR of Cassia tora leaves

Frequency cm^{-1}	Functional groups
3280.20	O-H
2919.03	C-H
1587.75	C=O
1247.11	C-O
1012.37	C-N

Table 3: FT-IR of Magnetic Sand

Frequency cm^{-1}	Functional groups
3749.71	**O-H**
1699.83	**C-H**
1542.17	**C=O**
1002.93	**C-O**
774.92	

C) XRD analysis of MnO_2 and magnetic sand

The result of the XRD analysis of MnO_2 as presented in Figure 1 shows the crystalline plane at various degree (211,101, 222, 400,210, 134, 220 and 002) which are well index to pure tetragonal structure according to JCPDS 10799 card. As shown in XRD component such full width high maximum (FWHM), the wavelength (d) in angstrom, and the 2 theta. These values were used to calculate the crystalline size and it can be seen from Figure 4 that the wavelength decreases as angle 2 theta increases.

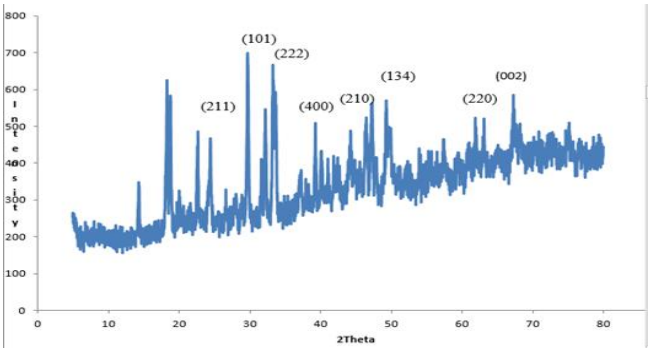

Figure 1: XRD spectrum of MnO_2

Figure 2 presented the XRD of the magnetic sand with full width maximum high (FWHM), wavelength (d) in angstrom and 2 theta that is angle of diffraction. These values were used in computing the size of the magnetic sand. Just like others the angle 2 theta increases with decreasing wavelength.

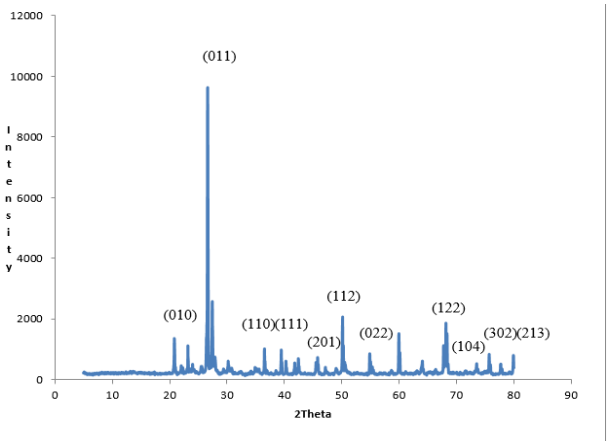

Figure 2: XRD spectrum of magnetic sand

D) The SEM of Manganese Oxide Nanoparticles

The scanning electron microscopic (SEM) analysis of the MnO_2 (Figure 3) solution control bioreduction from KMnO4 solution were early distinguishable from the lumps owing to their size differences. It was clear from the SEM picture shown in figure 6 that the manganese oxide nanoparticles exhibit agglomeration which occurred during the synthesis

ISSN (online): 2581-3048
Volume 7, Issue 12, pp 55-59, December-2023
https://doi.org/10.47001/IRJIET/2023.712007

process. It can be view that the MnNPs formed are moderately dispersed and slightly agglomerated. SEM images of those compounds had shown very clear that most of the particles are polymorphic morphology of material. The SEM image was very alike to that synthesized by [15].

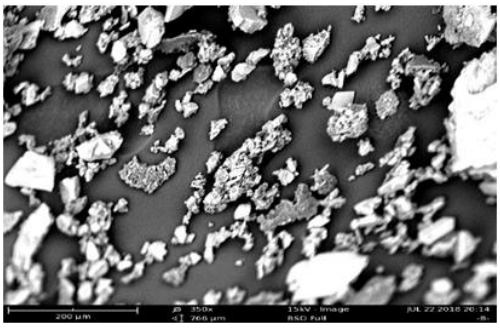

Figure 3: Scanning Electron Microscopy (SEM) of MnO_2

E) Photo-degradation of Methyl orange

The photodegradation of Methyl orange (MO) was used as a model to examine the photo-catalytic activity of the varied samples prepared herein. In a typical experiment, 0.6 mg/L of MO aqueous solution was prepared and 100 ml was measured into a conical flask. 0.6 mg of photocatalysts was mixed and put into a 100 mL conical flask. The photo-catalysts were ultrasonically dispersed in the flask, and the mixtures were then stirred for approximately 5 min. After this treatment, the flask was exposed to photo irradiation and stirred synchronously. A 300 W Hg arc lamp was used as the UV light source. The flask was then taken away from the light source after designated time intervals of 20 minutes and 10 ml of the mixtures was centrifuged to remove the catalysts. The remaining MO concentration was recorded by a Jenway 6405 UV–Vis Spectrophotometer [16]. The result of the Photo-catalytic activity of Magnetic Sand/Manganese Oxide as presented in Figure 7 which shows the variation of absorbance against time in minutes. The absorbance decreases as the time increases. This is visible in figure 8 is the plot of absorbance against time; a straight line was obtained with a good correlation coefficient (R2) of 0.9628.

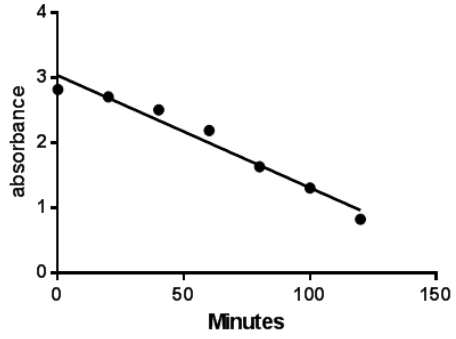

Figure 4: Photo-catalytic degradation of methyl orange by magnetic sand and manganese oxide nano-composite

IV. CONCLUSION

Manganese oxide nanoparticles were biosynthesized using *Cassia tora* aqueous leaf extract as the bioreducing agent that reduces potassium permanganate to manganese oxide which was characterized using UV-Visible spectrophotometer, FT-IR, SEM and XRD. The results show that the manganese oxide nanoparticles synthesized have an average size of 73 nm. Also magnetic sand nanoparticles were synthesized and characterized using UV-Visible spectrophotometer, FT-IR, XRF and XRD. The results show that the sand particle has about 70.16% SiO_2. Lastly, the photocatalytic ability of the nanocomposite was tested using methyl orange as a model and it was found that the nanocomposite was reversible as photocatalyst. This shows that the photodegradation of methyl orange follow a first order kinetic.

REFERENCES

[1] Ang, W., Li, X., Li, S., Yan-Jun, L., & Wei-Wei, L. (2013). CuO Nanoparticle Modified ZnO Nanorods with Improved Photocatalytic Activity. chin. phys. lett. Vol. 30, No. 4, 046202-5.

[2] Arora, A. K., Jaswal, V. S., Singh, K., & Singh, R. (2016). Applications of Metal/Mixed Metal Oxides as Photocatalyst: (A Review). Orient J Chem; 32(4).

[3] Farahmandjou, M., & Golabiyan, N. (2016). Synthesis and characterization of Alumina (Al_2O_3) nanoparticles prepared by simple sol-gel method. Int. J. Bio-Inorg. Hybr. Nanomater., 5(1): Spring 2016 , 73-77.

[4] Hang, N. Y. (2014). Photocatalytic Application of Metal Oxide Nanostructures. A dissertation submitted in partial fulfillment of the requirements for the degree of Master of Philosophy at The University of Hong Kong, 1-67.

[5] Jayandran, M., Muhamed, H., & Balasubramanian, V. (2015). Green synthesis and characterization of Manganese nanoparticles using natural plant extracts and its evaluation of antimicrobial activity. Journal of Applied Pharmaceutical Science Vol. 5 (12), 105-110.

[6] Kim, S., Choi, M., & Choi, H. (2016). Photocatalytic activity of SnO_2 nanoparticles in methylene blue degradation. Material Research and Bulleting Volume 74, 85-89.

[7] Kumar, H., Manisha, & Poonam, S. (2013). Synthesis and Characterization of MnO2 Nanoparticlesusing Co-precipitation Technique. International Journal of Chemistry and Chemical Engineering Volume 3, Number 3, 155-160.

[8] Kumar, V., Kulvinder, S., Shaily, P., & Surinder, K. M. (2017). Green synthesis of manganese oxide

ISSN (online): 2581-3048
Volume 7, Issue 12, pp 55-59, December-2023
https://doi.org/10.47001/IRJIET/2023.712007

nanoparticles for the electrochemical sensing of p-nitrophenol. Int Nano Lett (2017) 7, 123–131.

[9] Liua, R., Hub, P., & Chenb, S. (2012). Photocatalytic activity of Ag3PO4 nanoparticle/TiO_2 nanobelt heterostructures. Applied Surface Science 258, 9805–9809.

[10] Madheswaran, B. (2015). Synthesis and Characterization of Manganese Oxide Nanoparticles. New Delhi London Oxford New York Sydney: bloomsbury publishing india pvt. Ltd.

[11] Manigandan, R., Giribabu, K., Suresh, R., Munusamy, S., kumar, P. S., Muthamizh, S., et al. (2014). Characterization and Photocatalytic activity of Nickel oxide nanoparticles. International Journal of ChemTech Research CODEN: (USA) Vol.6, No.6, 3395-3398.

[12] Maryam, L., Gholamali, F., & Nasrin, E. (2014). Synthesis and surface modification of aluminum oxide nanoparticles. Journal of Ceramic Processing Research. Vol. 15, No. 5, 316-319.

[13] Mphilisi, M., Ngila, C., & Mamba, B. B. (2015). Recent Developments in Environmental Photocatalytic Degradation of Organic Pollutants: The Case of Titanium Dioxide Nanoparticles—A Review. Journal of Nanomaterials Volume 2015, 29.

[14] Oluwapelumi, O. O., Jonas, S. A., & Aderibigbe, D. (2017). Spectroscopic Characterization of a Nigerian Standard Sand: Igbokoda Sandi. International Journal of GEOMATE, Vol. 12, Issue 29, 89-98.

[15] Pandurang, V. D., VaideiBalraj, K., & Satish, D. K. (2018). Synthesis and Characterization of Aluminium Oxide (Al2O3) Nanoparticles and its Application in Azodye Decolourisation. International Journal of Environmental Chemistry 2018; 2(1), 10-17.

[16] Pathania, D., Rishu, K., & Harpreet, K. (2015). Enhanced photocatalytic activity of electrochemically synthesized aluminum oxide nanoparticles. 1-8.

Citation of this Article:

Charity Musa, Jeffrey T. Barminas, Shinggu D. Yamta, Janyo Noseh Dahiru, "Synthesis, Characterization and Photocatalytic Activity of MnO_2 and Magnetic Sand Composites" Published in *International Research Journal of Innovations in Engineering and Technology - IRJIET*, Volume 7, Issue 12, pp 55-59, December 2023. Article DOI https://doi.org/10.47001/IRJIET/2023.712007

****

